

Article

Effect of Refrigerated Inlet Cooling on Greenhouse Gas Emissions for a 250 MW Class Gas Turbine Engine

Ali Dinc , Ali Mamedov , Ertugrul Tolga Duran, Fethi Abbassi , Ibrahim Elbadawy , Kaushik Nag, Mehdi Moayyedean, Mohamed Fayed , Murat Otkur  and Yousef Gharbia

College of Engineering and Technology, American University of the Middle East, Egaila 54200, Kuwait; ali.mamedov@aum.edu.kw (A.M.); ertugrul.duran@aum.edu.kw (E.T.D.); fethi.abbassi@aum.edu.kw (F.A.); ibrahim.mohamed@aum.edu.kw (I.E.); kaushik.nag@aum.edu.kw (K.N.); mehdi.moayyedean@aum.edu.kw (M.M.); mohamed.fayed@aum.edu.kw (M.F.); murat.otkur@aum.edu.kw (M.O.); yousef.gharbia@aum.edu.kw (Y.G.)

* Correspondence: ali.dinc@aum.edu.kw; Tel.: +965-2225-1400

Abstract: In this study, the effect of inlet air cooling on greenhouse gas (GHG) emissions and engine performance for a land-based gas turbine engine was investigated under varying ambient temperatures (15–55 °C). The study aimed to reduce GHG emissions while improving output power and fuel efficiency during hot weather operating conditions. For illustrative purposes, a representative gas turbine engine model, approximating the 250 MW class General Electric (GE) engine, was analyzed in a simple cycle. A refrigeration process was integrated with a turboshaft gas turbine engine to chill the incoming air, and the power required for cooling was extracted from the gas turbine's output power. This mechanical chiller was assumed to provide a 15 °C inlet air temperature. Without inlet air cooling, at 55 °C ambient temperature, the engine's power output was calculated to decrease by 15.06%, while power-specific fuel consumption and GHG emissions increased by 6.09% and 5.84%, respectively. However, activating the refrigeration or cooling system in the inlet made it possible to mitigate most of the adverse effects of hot weather on the engine's performance and GHG emissions. Therefore, with inlet air cooling, the power output loss reduces to 3.28%, indicating an 11.78% recovery compared to the 15.06% loss without cooling. Similarly, the rise in power-specific fuel consumption caused by high ambient temperature decreases from 6.09% to 3.43%, reflecting a 2.66% improvement. An important finding of the study is that with inlet air cooling, the increase in GHG emissions reduces from 5.84% to 3.41%, signifying a 2.43% improvement on a hot day with a temperature of 55 °C.

Keywords: inlet air cooling; gas turbine engine; exhaust emissions; global warming potential; sustainability



Citation: Dinc, A.; Mamedov, A.; Duran, E.T.; Abbassi, F.; Elbadawy, I.; Nag, K.; Moayyedean, M.; Fayed, M.; Otkur, M.; Gharbia, Y. Effect of Refrigerated Inlet Cooling on Greenhouse Gas Emissions for a 250 MW Class Gas Turbine Engine. *Aerospace* **2023**, *10*, 833. <https://doi.org/10.3390/aerospace10100833>

Academic Editor: Jian Liu

Received: 22 May 2023

Revised: 1 September 2023

Accepted: 6 September 2023

Published: 25 September 2023



Copyright: © 2023 by the authors. Licensee MDPI, Basel, Switzerland. This article is an open access article distributed under the terms and conditions of the Creative Commons Attribution (CC BY) license (<https://creativecommons.org/licenses/by/4.0/>).

1. Introduction

Human-related activities, such as energy production, transportation, and heating, that are heavily reliant on fossil fuels are contributing to an increasing amount of greenhouse gases. These emissions, in turn, exacerbate anthropogenic global warming. The energy sector commonly employs land-based gas turbines in various countries. For example, Gulf Cooperation Council (GCC) countries like Kuwait, Saudi Arabia, Bahrain, Oman, Qatar, and the United Arab Emirates heavily rely on gas turbine engines for electric power generation. In Saudi Arabia, gas turbine engines account for approximately 42% of the total electric power generation. Similarly, Kuwait has significant investments in gas turbines for electricity production, with the Sabiya West gas-fired power plant being one of its largest power stations, utilizing a combined-cycle approach. It has a capacity of producing 5.866 MW (31.1%) of the total 18.838 MW of electric power for Kuwait in 2018 [1] and is equipped with gas turbines along with steam turbines [2].

In hot climates, the performance of gas turbines degrades as the ambient temperature increases. The GCC region, in particular, experiences extremely high temperatures, especially during the summer when electricity demand peaks due to air-conditioning requirements. Consequently, gas turbine engines face performance losses in such hot ambient conditions. For this study, a land-based gas turbine model, the General Electric (GE) MS9001 (PG9351FA) model, was chosen as a case study. The GE MS9001 series gas turbines are single-shaft heavy-duty combustion turbines designed to produce 250+ MW (with an efficiency of 37–38%) in a simple cycle and 400+ MW (with an efficiency of 59–60%) in a combined-cycle configuration. The GE MS9001 model is one of the gas turbine types employed in the power plant at Sabiya, Kuwait. In one of the reports by GE Power Systems, a leading manufacturer of gas turbine engines, Brooks [3] depicted the effect of ambient temperature for the MS7001 model engine on various parameters, including power output, as shown in Figure 1. Due to its nature as an air-breathing engine, the gas turbine's performance is influenced by factors impacting the density and mass flow of the air intake into the compressor. Therefore, some performance changes occur in ambient weather conditions, which deviate from the reference conditions of 15 °C and 1.013 bar. It is essential to note that each turbine model has its own distinct temperature-effect curve, as it relies on the specific cycle it operates on.

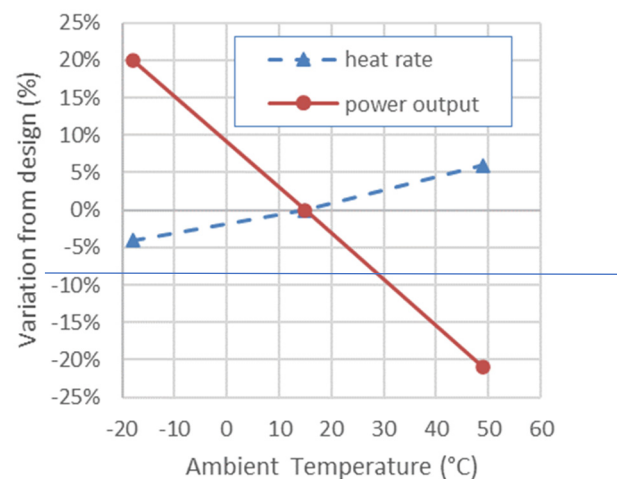


Figure 1. Effect of ambient temperature on MS7001 engine performance (adopted from [3]).

De Sa and AlZubaidy [4] conducted a study on particular gas turbines (SGT 94.2 and SGT 94.3) installed in the Dubai region. They examined the performance of these engines under different ambient temperatures and found that the power output, which was 265 MW at 15 °C, reduced to 220.35 MW (a decrease of 17%) at 45 °C. This implies that for every 1 °C increase in ambient temperature above ISO conditions, the units experience a reduction of 0.1% in thermal efficiency and 0.553% in total power output.

To address the performance degradation resulting from hot ambient air conditions, several inlet air cooling technologies are available for applications such as evaporative cooling, absorption chillers, and mechanical chillers. A refrigeration or cooling system is a broad term used to describe any system that removes heat from a space or substance to lower its temperature. A chiller is a specific type of refrigeration system used to cool a liquid (usually water or a water–glycol mixture) that can then be used to cool air or equipment. Fogging is an evaporative cooling technique that involves the introduction of a fine mist or fog of water into the air. When the water droplets evaporate, they absorb heat from the surrounding air, reducing its temperature. In this study, a mechanical chiller was considered a refrigeration system in the inlet because of its simplicity. In the literature, there are numerous studies available on inlet air cooling. Arabi et al. [5] presented a detailed evaluation of a gas turbine that used inlet air cooling. In the presented study, the authors employed GE type F5 gas turbines for energy analysis. Barigozzi et al. [6] performed an

economical and technical evaluation of a power plant with combined inlet air cooling and a gas turbine for various climatic conditions. Bassily [7] studied enhancements on intercooling, reheating, and recuperation on gas turbine cycles, where he evaluated evaporative after-cooling and absorption-type inlet air cooling as performance enhancements for the mentioned turbine cycle. Chase and Kehoe [8] discussed the use of evaporative and mechanical chiller systems for gas turbine inlet air cooling. Chen et al. [9] established a thermodynamic optimization for a gas turbine with a refrigeration cycle to cool the inlet air in a power plant. De Lucia et al. [10] compared the effectiveness of multiple solutions to cool the inlet air of a gas turbine for a cogeneration facility. Farzaneh-Gord et al. [11] proposed an innovative technique of inlet air cooling to increase the efficiency of an industrial gas turbine.

GE Gas Power [12] has already developed commercial inlet air chilling systems for the market. Similarly, Stellar Energy [13] has developed and installed turbine inlet air cooling systems to cater to customers with power generation plants operating in high ambient temperatures. Stellar Energy offers up to 35% output gains with its gas turbine inlet air chilling systems. Kodituwakku [14] calculated the impact of inlet air cooling and estimated the viability of inlet air cooling in the “Kelanitissa” gas turbine power plant for performance. Loud and Slaterpryce [15] explained basic inlet air treatment methods, including inlet air cooling for gas turbines. According to a report by GE Power Systems, Johnston [16] explained that evaporative coolers can result in power increases of up to 14% in hot, dry ambient conditions. Malewski and Holldorff [17] examined the enhancement of gas turbine power output by using exhaust heat waste to pre-cool the input air via absorption refrigeration. Mohapatra and Sanjay [18] conducted a parametric study of two separate methods of air cooling at the inlet for gas turbines. Najjar [19] looked at the potential improvement in the thermal efficiency of a gas turbine engine by introducing a precooler to the evaporator for inlet air cooling. Najjar and Al-Zoghool [20] studied four different inlet air cooling systems to make comparisons of the performance parameters for proposing the most sustainable technique for gas turbine engines. Omar Kamal et al. [21] conducted research on the feasibility of utilizing mechanical chillers to cool the inlet air for turbines in the high ambient temperatures of Malaysia’s climate. Potnis and Joshi [22] obtained a patent for a system that enhances the effectiveness and performance of turbines by cooling incoming air. Rahim [23] analyzed multiple methods of inlet air cooling and calculated their effects on a gas turbine’s performance and its sensitivity in a combined cycle. Sanaye et al. [24] employed a cooling process on the inlet air for a gas turbine using a latent thermal energy (from ice) storage system and optimized it in terms of capital and operating costs. Wang and Chiou [25] researched how to integrate steam injection and intake air cooling in a gas turbine generation system. Yang et al. [26] suggested a systematic approach for the assessment of the application of inlet air chilling and fogging by utilizing absorption chillers and evaporative fogging in a power plant using a combined cycle. Zurigat et al. [27] conducted research on the technological viability of using ice or water (thermal energy storage) in order to decrease the temperature of the inlet air for a gas turbine located in an oil field.

CO₂ and NO_x are among the major exhaust gases contributing to global warming, especially considering the operational flights of both manned and unmanned aerial vehicles (UAVs). Dinc [28] analyzed the effect of polytropic efficiency and compressor pressure ratio on power-specific fuel consumption and exhaust gases. Dinc and Elbadawy [29] investigated the GWP effect for a turbofan-propelled UAV throughout a surveillance flight with a wide altitude range for different Mach numbers. The GWP effect was calculated considering CO₂, H₂O, and NO_x emissions. Optimization of flight altitude and vehicle speed-related Mach numbers resulted in 13 km and 0.37, respectively, for the best-case scenario. In a later study, Dinc [30] examined the design parameters of a turbofan engine, such as turbine inlet temperature, flight Mach number, compressor and booster pressure ratios, isentropic efficiencies, and power and high-pressure turbine isentropic efficiencies. Analysis proved that turbine inlet temperature has the highest sensitivity value, and

isentropic efficiencies of boosters and compressors have the lowest sensitivity values. Internal combustion engines (ICEs) are also widely used, especially for small UAVs, and their effects on GWP also need to be investigated. Dinc and Otkur [31] analyzed the surveillance flight of an MQ-1 B “Predator-A” UAV propelled with a Rotax 912 ICE engine using AVGAS 100LL airplane fuel. As gas turbine engines are frequently used for power generation, especially in the GCC countries, Dinc and Gharbia [32] conducted an analysis study of similar design parameters to calculate global warming impact of a 43 MW class land based gas turbine engine. Inlet air temperature acts as a significant factor in the power values of gas turbines, and Dinc et al. [33] analyzed the hot climate performance decrease of a gas turbine engine in the 43 MW class and concluded that at 55 °C, there is a 21.3% reduction in the generated power and a 9.31% increase in power-specific fuel consumption (PSFC). Dinc et al. [34] introduced air inlet air cooling with a refrigeration system to the same gas turbine and obtained the normal ambient temperature power values with a PSFC improvement of 5.2% compared to the uncooled case. Additional studies on engine emissions can be found in the literature [35–38].

2. Materials and Methods

In this study, the effect of refrigerated inlet air cooling on greenhouse gas (GHG) emissions and on the performance of a land-based gas turbine engine is investigated in a range of ambient temperatures (15–55 °C).

2.1. Refrigerated Inlet Air Cooling Model

In this study, a refrigeration cycle is integrated with a turboshaft gas turbine engine to cool the inlet air. The necessary power for refrigeration has been sourced from the mechanical power output of the gas turbine, as depicted in Figure 2. This mechanical chiller (cooler) is assumed to provide a 15 °C inlet air temperature at all times.

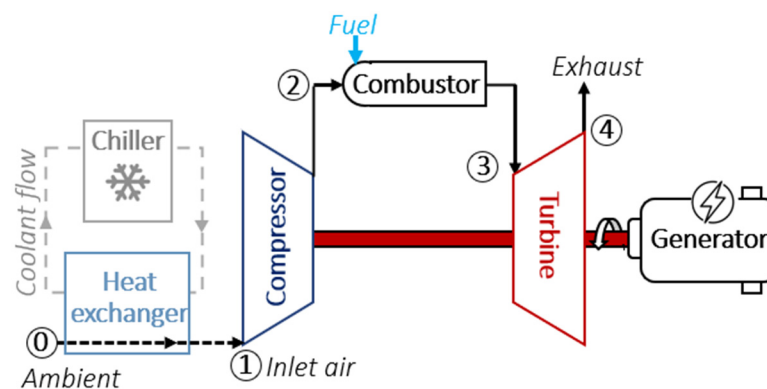


Figure 2. Schematic view of refrigerated inlet air cooling for a gas turbine.

General equations for inlet air cooling and engine performance are given in Equations (1)–(11). Equation (1) is used to calculate the cooling load or heat removed from the inlet of the engine, \dot{Q}_{cool} , for the purpose of cooling, where, \dot{m}_a and h are the air mass flow rate [kg/s] and the enthalpy [kJ/kg], respectively. Then, W_{cool} work input for the mechanical chiller can be calculated using Equation (2) where COP is the coefficient of performance of the chiller (refrigeration system).

In this study, the specific selection of a refrigerant gas was not the primary objective. However, it is worth noting that various gases used today are applicable for refrigeration purposes. In this investigation, a typical coefficient of performance (COP) value of 3.0 was assumed. Common refrigerants used in refrigerators include R-134a, R-600a (isobutane), R-290 (propane), and R-22, among others. Nevertheless, the environmental impact of these refrigerant gases, particularly in terms of their global warming potential (GWP) and ozone-depleting potential, must be thoroughly evaluated before making a definitive choice. Sustainable and eco-friendly refrigerant options are being emphasized to reduce

the environmental footprint of refrigeration systems. The power required to drive the compressor, \dot{W}_C , is calculated from Equation (3). Then, the amount of heat of fuel from the combustor, \dot{Q}_{in} , is calculated using Equation (4), and the required fuel mass flow rate, \dot{m}_f can be found using Equation (5), where η_b is the burner efficiency and LHV is the lower heating value of fuel (natural gas or methane used in this study).

$$\dot{Q}_{cool} = \dot{m}_a \cdot (h_1 - h_0) \quad (1)$$

$$\dot{W}_{cool} = \frac{\dot{Q}_{cool}}{COP} \quad (2)$$

$$\dot{W}_C = \dot{m}_a \cdot (h_2 - h_1) \quad (3)$$

$$\dot{Q}_{in} = \dot{m}_a \cdot (h_3 - h_2) \quad (4)$$

$$\dot{m}_f = \frac{\dot{Q}_{in}}{\frac{LHV}{\eta_b}} \quad (5)$$

2.2. Gas Turbine Engine Performance Model

A comprehensive cycle analysis was conducted, involving thermodynamic calculations for all engine components, including the intake compressor, combustion chamber, turbine, and more. The study meticulously determined total pressure and temperature values at various engine stations, subsequently evaluating overall performance parameters such as fuel consumption, heat rate, and power output. Additionally, exhaust emissions were accurately calculated based on these values.

The foundation of this research was a representative gas turbine engine model closely resembling the General Electric MS9001FA (PG9351FA) engine of the 250 MW class, analyzed in a simple cycle. The input parameters were carefully considered to derive and present the overall performance parameters. Comparisons with data from manufacturers in the literature reveal that the results obtained in this study exhibit a maximum deviation of 1% for ISO base rating power (kW), heat rate (kJ/kWh), exhaust temperature (°C), and exhaust flow (kg/s), as shown in Table 1.

Table 1. Comparison of the engine performance model with manufacturer data.

Parameter	Manufacturer Data [3]	Calculation	Deviation
ISO Base Rating (kW)	255,600	257,310	0.64%
Heat Rate (kJ/kWh)	9757	9725	−0.31%
Exhaust Flow (kg/s)	643.89	643.57	−0.05%
Exhaust Temp. (°C)	608	610.5	0.42%

Calculations of GHG emissions from an engine require typical parameters such as power, fuel consumption, temperature, pressure values, etc. A summary of engine performance equations is given as follows [39]. Equation (6) is used to calculate the output power of the turbine, \dot{W}_T , and Equation (7) gives the total mass inlet to the turbine \dot{m}_T , which is the summation of air and fuel mass flow rates. The net shaft power delivered \dot{W}_{net} and the power-specific fuel consumption $PSFC$ are calculated using Equation (8) and Equation (9), respectively. Heat rate HR for the engine is computed using Equation (10), and finally, thermal efficiency η_{th} is calculated using Equation (11).

$$\dot{W}_T = \dot{m}_T \cdot (h_4 - h_3) \quad (6)$$

$$\dot{m}_T = \dot{m}_a + \dot{m}_f \quad (7)$$

$$\dot{W}_{net} = \dot{W}_T - \dot{W}_C - \dot{W}_{cool} \quad (8)$$

$$PSFC = \frac{3600 \cdot \dot{m}_{fuel}}{\dot{W}_{net}} \quad (9)$$

$$HR = PSFC \cdot LHV \quad (10)$$

$$\eta_{th} = \frac{3600}{PSFC \cdot LHV} \quad (11)$$

2.3. Global Warming Potential Model

In the next step, exhaust gases that contribute to global warming, such as carbon dioxide, nitrogen oxides, etc., are calculated, as these gases collectively add up to the greenhouse gas (GHG) value. The impact of CO₂ produced during the combustion process holds significant importance, as it serves as the primary contributor to global warming. The global warming potential (GWP) serves as a metric to gauge the environmental harm caused by a greenhouse gas on Earth. This measurement is relative to the warming effect caused by a specific amount of CO₂ (GWP of 1kg CO₂ = 1). Greenhouse gases have long-lasting effects, and the assessment of their impact is conducted over a specific time span. In this context, a time interval of 100 years is chosen for evaluating the damage caused by these gases (GWP₁₀₀). Water vapor's impact is commonly disregarded at sea level, and emissions of H₂O gas are expected to have a negligible effect [40]. According to Svensson et al. [41], up to 10 km altitude, the contribution of H₂O to global warming is insignificantly small in comparison to that of CO₂. However, at altitudes above 10 km, it does have a minor but increasing impact on global warming (considering cruising aircraft). Global warming potential (GWP₁₀₀, cumulative forcing over 100 years) numbers for several gases are given in Table 2.

NOx emissions, which consist of both NO and NO₂ [42], are released from the combustion process in engines and lead to a range of undesirable environmental consequences. Presently, the scientific community is engaged in a debate regarding the influence of NOx on the greenhouse effect (GHE). Certain scientists unequivocally categorize NOx as a greenhouse gas (GHG), considering it on par with direct GHGs like CO₂, CH₄, N₂O, and hydrofluorocarbons (HFCs). While N₂O is part of the category of direct greenhouse gases (GHGs), it should not be categorized as NOx [43].

Table 2. Global warming potential values of several gases [43–45].

Gas	GWP ₁₀₀
CO ₂	1
NOx	1.6 *
	10 **
CH ₄	28
N ₂ O	265
CF ₄	6630

* Realistic scenario; ** Pessimistic scenario [43,44].

The GHG emissions can be calculated using Equations (12)–(15). In Equation (12), we can assume that the total GHG emissions are the sum of CO₂ and NOx produced during the combustion process in the gas turbine, ignoring other minor contributors. Equation (13) gives the CO₂ emission, which is the emission index (EI) (EI_{CO₂} = 2.75 kg/kg fuel for natural gas or methane) [46] multiplied by the fuel flow rate (\dot{m}_f). It means that, when one kilogram of fuel is burned, approximately 2.75 kg of CO₂ are produced during the combustion process of methane. The calculation of NOx emissions is more complex and requires correlation with test data, if available. By the engine manufacturer (GE Power

Systems), test data for NO_x are given as 162 ppmv (~323 kg/h) at 15% O₂ for the MS9001E engine using natural gas as fuel and in dry configuration (various configurations involving different fuels and combustors lead to the existence of diverse NO_x values published by the engine manufacturer) [16,47]. Additionally, in a report by the manufacturer, NO_x emissions of a similar gas turbine engine vs. ambient temperature were plotted [16]. Combining several sets of manufacturer data and the typical NO_x trend suggested by Hung et al. [48], a NO_x emission model was obtained and is depicted in Figure 3. In Figure 3, the solid part of the curve is based on manufacturer data, and the dotted part is the extrapolation by a polynomial curve fit. Then, this NO_x model was added to the GHG calculations.

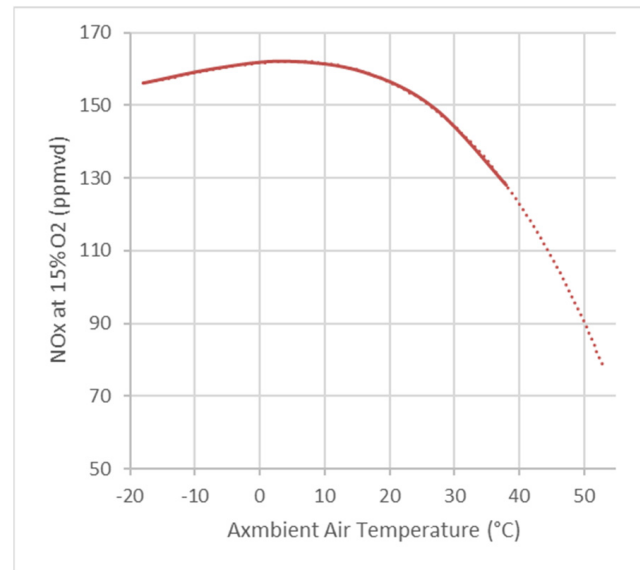


Figure 3. NO_x emissions of a gas turbine engine (adopted from [16,48]).

In Equation (14), NO_x emissions are expressed as an equivalent of CO₂ over a specified time horizon (100 years) to assess their impact on the greenhouse effect. The literature indicates an ongoing discussion concerning the global warming potential (GWP) values for NO_x. Lasek et al. [43] have highlighted variations in GWP for NO_x in different studies, attributed to geographical locations and altitudes, leading to both negative and positive GWP values. To address this uncertainty, two scenarios for $GWP_{NOx-100}$ values (1.6 for the realistic scenario and 10 for the pessimistic scenario) were considered, as suggested by Lasek et al. [43] and presented in Table 2. For this study, a GWP value of 1.6 was selected, reflecting the realistic scenario. The NO_x emissions produced by the engine (GHG_{NOx}) were calculated by approximating the test data provided by the manufacturer (Figure 3). Subsequently, the total GHG emissions (in CO₂ equivalent) were calculated using Equation (15), which involves summing up the CO₂ and NO_x emissions and then multiplying them by their respective GWP_{100} values. In the literature, the GWP_{100} value for CO₂ is equal to 1.

$$GHG_{tot} = GHG_{CO_2} + GHG_{NOx} \quad (12)$$

$$GHG_{CO_2} = EI_{CO_2} \dot{m}_f \quad (13)$$

$$GHG_{NOx-eq.CO_2} = GHG_{NOx} GWP_{NOx-100} \quad (14)$$

$$GHG_{tot-eq.CO2} = GHG_{CO2} GWP_{CO2-100} + GHG_{NOx} GWP_{NOx-100} \quad (15)$$

3. Results and Discussion

The results can be summarized in two parts for the investigated ambient temperature interval (15–55 °C). As shown in Figure 2 earlier, this study proposes the use of a mechanical chiller, which utilizes a portion of the engine's output power for inlet air cooling/refrigeration when active in the engine's inlet, to provide a 15 °C inlet temperature.

The first part of the summary pertains to the effect of intake refrigeration on the engine's performance, while the second part focuses on the impact on greenhouse gas (GHG) emissions. All effects on performance parameters and GHG are tabulated in Tables 3 and 4 and presented in Figures 4–19. The summary of results is considered at ambient temperatures of up to 55 °C.

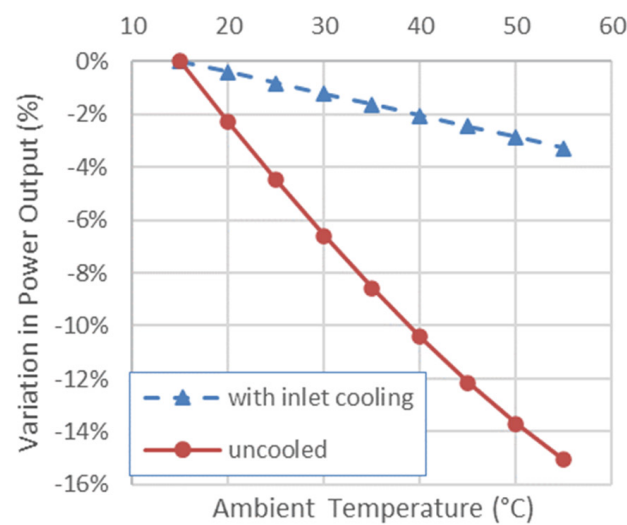


Figure 4. Variation in power output (%).

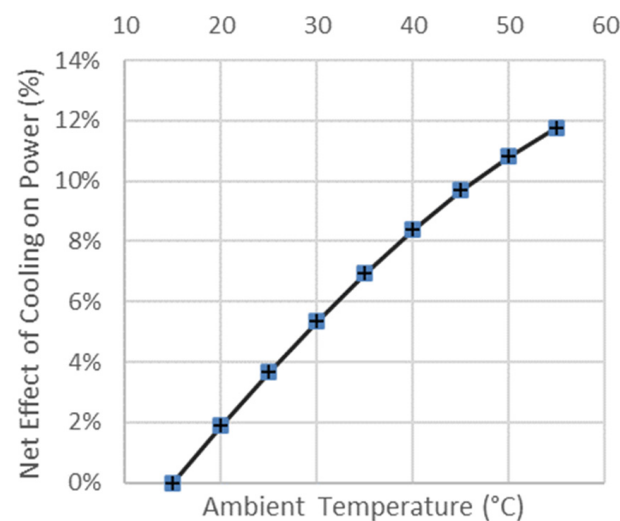


Figure 5. Net effect of inlet air cooling on power (%).

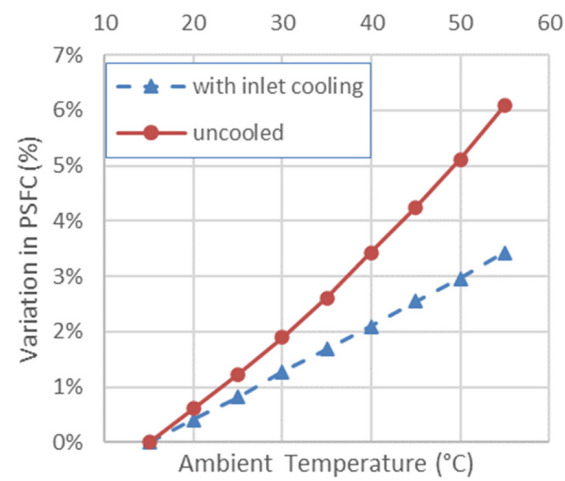


Figure 6. Variation in PSFC (%).

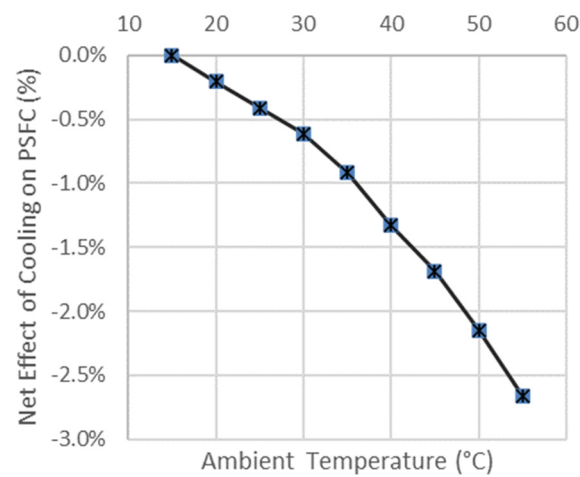


Figure 7. Net effect of inlet air cooling on PSFC (%).

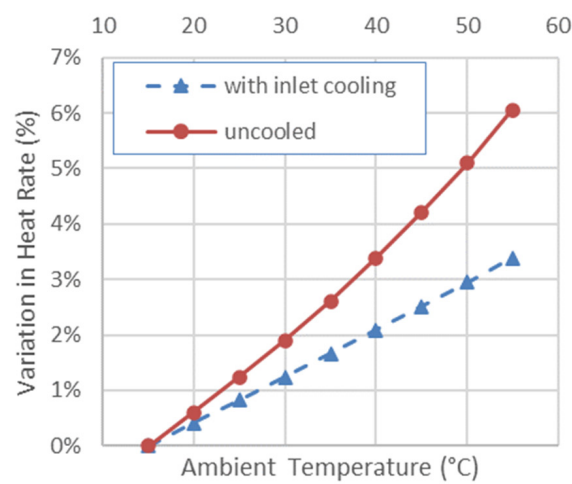


Figure 8. Variation in heat rate (%).

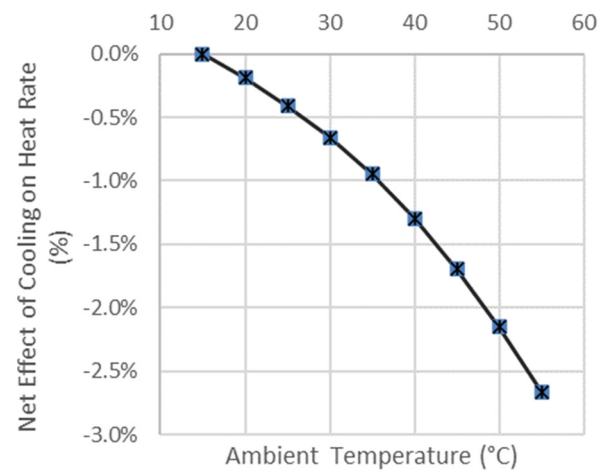


Figure 9. Net effect of inlet air cooling on heat rate (%).

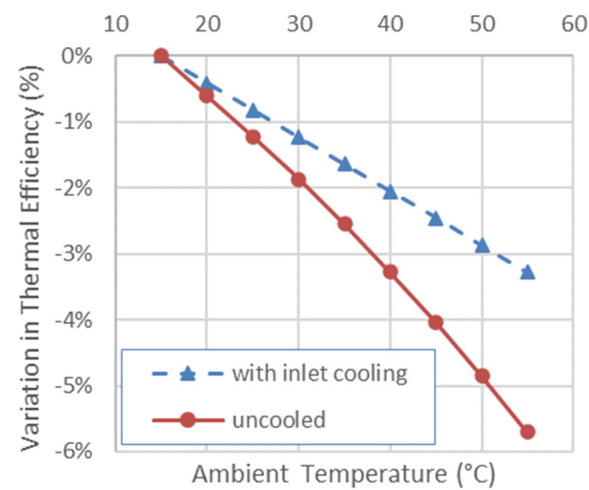


Figure 10. Variation in thermal efficiency (%).

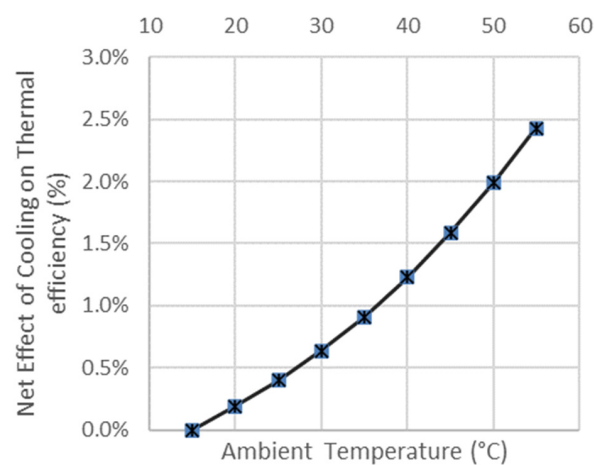


Figure 11. Net effect of inlet air cooling on thermal efficiency (%).

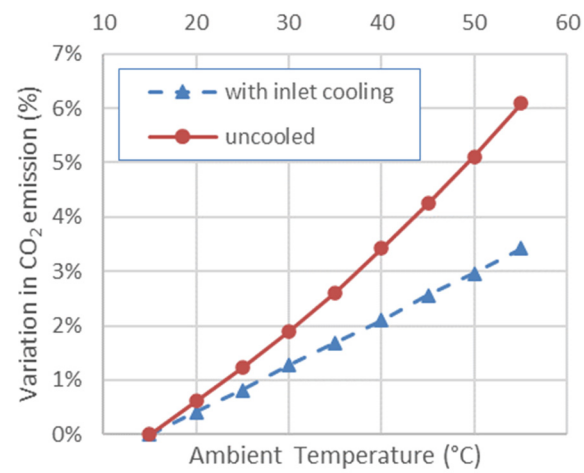


Figure 12. Variation in CO₂ emissions (%).

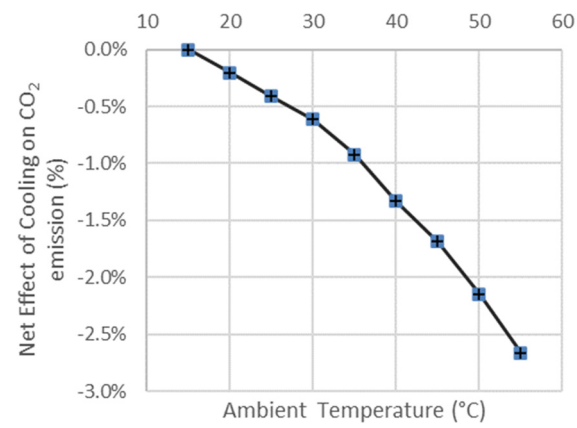


Figure 13. Net effect of inlet air cooling on CO₂ emissions (%).

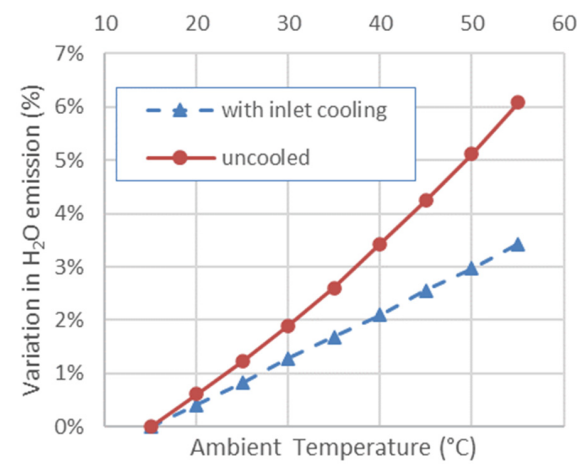


Figure 14. Variation in H₂O emissions (%).

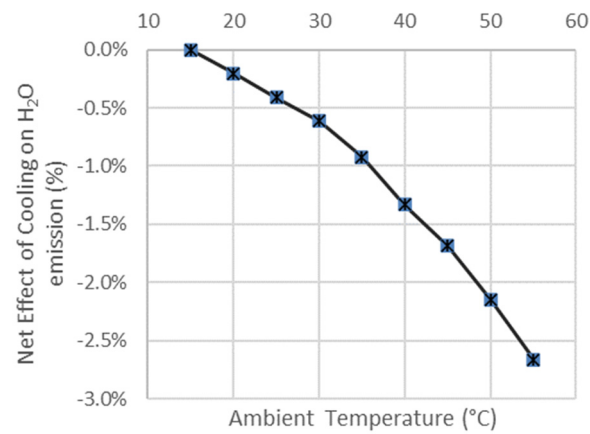


Figure 15. Net effect of inlet air cooling on H₂O emissions (%).

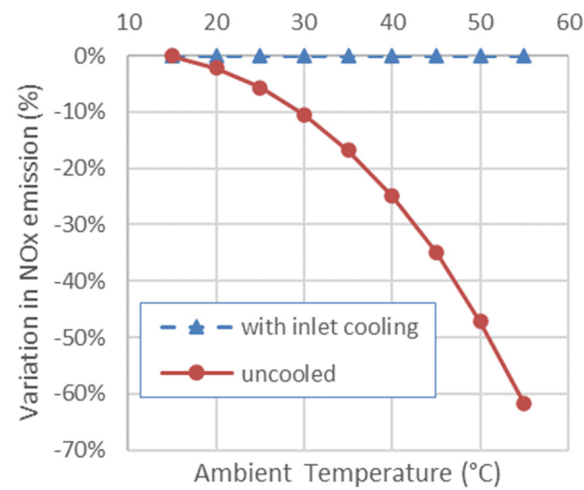


Figure 16. Variation in NOx emissions (%).

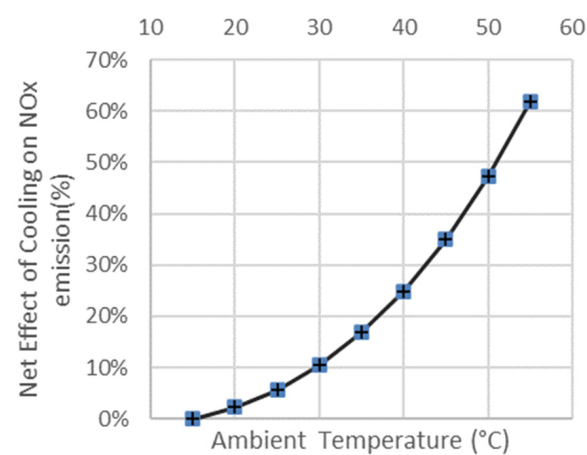


Figure 17. Net effect of inlet air cooling on NOx emissions (%).

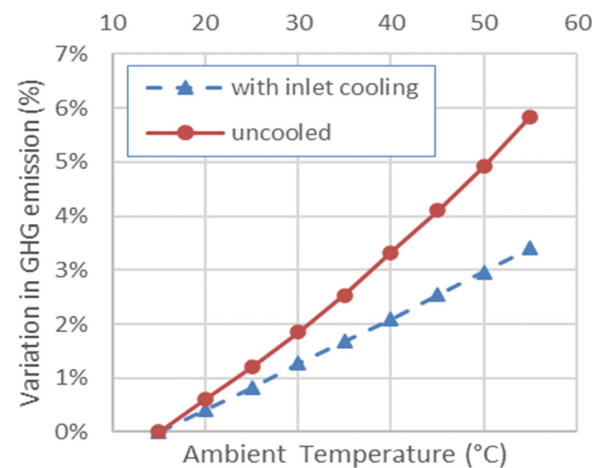


Figure 18. Variation in total GHG emissions (%).

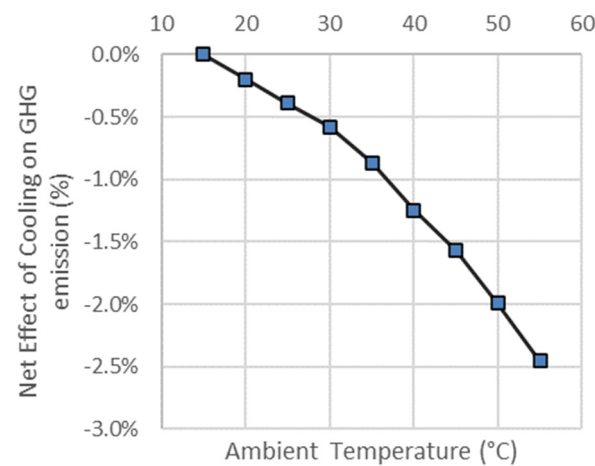


Figure 19. Net effect of inlet air cooling on total CO₂ equivalent GHG emissions (%).

At 55 °C, the engine's performance experiences a degradation of 15.06% in power output (Figure 4, red curve: uncooled). However, it is possible to recover some of the power loss through inlet air cooling (Figure 4, blue curve: with inlet air cooling). The refrigeration system or mechanical chiller effectively recovers most of the performance degradation, resulting in a power output loss of only 3.28% (Figure 4) instead of 15.06%, amounting to an 11.78% recovery. Figure 5 illustrates the difference between the power output change curve for an engine with air cooling (blue curve in Figure 4) and the power output change curve for an engine running with no air cooling (red curve in Figure 4), reaffirming the 11.78% recovery. Inlet air cooling proves to be highly effective in recovering most of the power output losses at 55 °C.

Hot ambient conditions lead to another adverse effect on power-specific fuel consumption, resulting in a 6.09% increase at 55 °C (Figure 6). However, this rise in power-specific fuel consumption (PSFC) can be mitigated by inlet air cooling, reducing it to 3.43% and leading to a notable 2.66% improvement. In essence, inlet air cooling enhances PSFC by up to 2.66% (Figure 7). In other words, cooling the inlet air for the engine reduced the PSFC at 55 °C by 2.66% compared to an engine where there is no inlet air cooling.

Table 3. Effect of ambient temperature and inlet air cooling on the performance of the engine.

Ambient Temperature °C	Inlet Temperature °C	Configuration	Power (kW)	Power Change from 15 °C ISO Day	Power Change from Hot Ambient	PSFC (kg/(kW x h))	PSFC Change from 15 °C ISO Day	PSFC Change from Hot Ambient	Heat Rate (kJ/(kW x h))	Heat Rate Change from 15 °C ISO Day	Thermal Efficiency	Thermal Eff. Change from ISO Day
15	15	ISO day	257,310	0.00%		0.1955	0.00%		9725	0.00%	37.02%	0%
20	15	cooled to 15 °C	256,255	−0.41%	1.88%	0.1963	0.41%	−0.20%	9765	0.41%	36.87%	−0.41%
20	20	uncooled	251,413	−2.29%		0.1967	0.61%		9783	0.60%	36.80%	−0.60%
25	15	cooled to 15 °C	255,201	−0.82%	3.67%	0.1971	0.82%	−0.41%	9805	0.83%	36.72%	−0.82%
25	25	uncooled	245,763	−4.49%		0.1979	1.23%		9845	1.23%	36.57%	−1.22%
30	15	cooled to 15 °C	254,147	−1.23%	5.36%	0.1980	1.28%	−0.61%	9846	1.24%	36.56%	−1.23%
30	30	uncooled	240,366	−6.58%		0.1992	1.89%		9910	1.90%	36.33%	−1.87%
35	15	cooled to 15 °C	253,093	−1.64%	6.93%	0.1988	1.69%	−0.92%	9887	1.67%	36.41%	−1.64%
35	35	uncooled	235,259	−8.57%		0.2006	2.61%		9979	2.61%	36.08%	−2.55%
40	15	cooled to 15 °C	252,038	−2.05%	8.38%	0.1996	2.10%	−1.33%	9928	2.09%	36.26%	−2.05%
40	40	uncooled	230,485	−10.43%		0.2022	3.43%		10,054	3.39%	35.81%	−3.28%
45	15	cooled to 15 °C	250,983	−2.46%	9.68%	0.2005	2.56%	−1.69%	9970	2.52%	36.11%	−2.46%
45	45	uncooled	226,078	−12.14%		0.2038	4.25%		10,135	4.22%	35.52%	−4.05%
50	15	cooled to 15 °C	249,930	−2.87%	10.82%	0.2013	2.97%	−2.15%	10,012	2.95%	35.96%	−2.87%
50	50	uncooled	222,087	−13.69%		0.2055	5.12%		10,221	5.10%	35.22%	−4.85%
55	15	cooled to 15 °C	248,875	−3.28%	11.78%	0.2022	3.43%	−2.66%	10,054	3.39%	35.81%	−3.28%
55	55	uncooled	218,566	−15.06%		0.2074	6.09%		10,313	6.05%	34.91%	−5.71%

Table 4. Effect of ambient temperature and inlet air cooling on the emissions of greenhouse gases.

Ambient Temperature °C	Inlet Temperature °C	Configuration	CO ₂ (kg/(kW x h))	CO ₂ Change from 15 °C ISO Day	H ₂ O (kg/(kW x h))	H ₂ O Change from 15 °C ISO Day	CO ₂ and H ₂ O Change from Hot Ambient	NOx (g/(kW x h))	NOx Change from 15 °C ISO Day	NOx Change from Hot Ambient	GHG _{tot-eq.CO2} (kg/(kW x h))	GHG _{tot-eq.CO2} Change from ISO Day	GHG _{tot-eq.CO2} Change from Hot Ambient
15	15	ISO day	0.617	0.00%	0.440	0.00%		1.236	0.00%		0.540	0%	
20	15	cooled to 15 °C	0.54	0.41%	0.442	0.41%	−0.20%	1.236	0.00%	2.21%	0.542	0.41%	−0.20%
20	20	uncooled	0.541	0.61%	0.443	0.61%		1.209	−2.21%		0.543	0.60%	
25	15	cooled to 15 °C	0.542	0.82%	0.443	0.82%	−0.41%	1.236	0.00%	5.61%	0.544	0.82%	−0.39%
25	25	uncooled	0.544	1.23%	0.445	1.23%		1.167	−5.61%		0.546	1.20%	
30	15	cooled to 15 °C	0.545	1.28%	0.446	1.28%	−0.61%	1.236	0.00%	10.41%	0.546	1.27%	−0.57%
30	30	uncooled	0.548	1.89%	0.448	1.89%		1.108	−10.41%		0.55	1.85%	
35	15	cooled to 15 °C	0.547	1.69%	0.447	1.69%	−0.92%	1.236	0.00%	16.78%	0.549	1.68%	−0.86%
35	35	uncooled	0.552	2.61%	0.451	2.61%		1.029	−16.78%		0.553	2.54%	
40	15	cooled to 15 °C	0.549	2.10%	0.449	2.10%	−1.33%	1.236	0.00%	24.92%	0.551	2.09%	−1.23%
40	40	uncooled	0.556	3.43%	0.455	3.43%		0.928	−24.92%		0.558	3.32%	
45	15	cooled to 15 °C	0.551	2.56%	0.451	2.56%	−1.69%	1.236	0.00%	35.01%	0.553	2.55%	−1.55%
45	45	uncooled	0.56	4.25%	0.459	4.25%		0.804	−35.01%		0.562	4.10%	
50	15	cooled to 15 °C	0.554	2.97%	0.453	2.97%	−2.15%	1.236	0.00%	47.23%	0.556	2.96%	−1.97%
50	50	uncooled	0.565	5.12%	0.462	5.12%		0.652	−47.23%		0.566	4.92%	
55	15	cooled to 15 °C	0.556	3.43%	0.455	3.43%	−2.66%	1.236	0.00%	61.79%	0.558	3.41%	−2.43%
55	55	uncooled	0.57	6.09%	0.467	6.09%		0.472	−61.79%		0.571	5.84%	

In Figure 8, the impact of ambient temperature on heat rate is depicted. The heat rate represents the quantity of energy required by an engine or power plant to produce one kilowatt-hour (kWh) of power output. A higher ambient temperature results in greater energy input (fuel consumption) for the same power output. Likewise, Figure 9 demonstrates the favorable effects of inlet air cooling on heat rate.

In a similar vein, as ambient temperature rises (as depicted in Figure 10), the thermal efficiency experiences a decrease. However, the application of inlet air cooling proves to be instrumental in aiding the recovery of thermal efficiency, as demonstrated in Figure 11. In hotter conditions, the engine requires more energy (fuel) to operate, resulting in reduced thermal efficiency. However, when the inlet air cooling mechanism is activated, the incoming air is chilled, mitigating the adverse effects of high ambient temperatures.

As a consequence of the increased fuel consumption at high ambient conditions, CO₂ emissions in (kg/(kW × h)) show an increase of up to 6.09%, but when inlet air cooling is applied, the increase in CO₂ emissions is reduced to 3.43% (as indicated in Figures 12 and 13). This effect can be attributed to the combustion process, where approximately 2.75 kg of CO₂ and 2.25 kg of H₂O are produced for every kilogram of natural gas or methane burned.

Although water vapor (H₂O) was not incorporated into the overall greenhouse gas (GHG) calculations, it was nevertheless calculated as a part of exhaust emissions and depicted in Figures 14 and 15. Notably, H₂O exhibits a similar trend to CO₂, as both emissions are directly related to the quantity of fuel burned during the combustion process.

The relationship between CO₂ and H₂O emissions and fuel consumption underscores the importance of effectively managing fuel usage to minimize the environmental impact. As these emissions are inherently linked to the combustion process, measures such as inlet air cooling can play a crucial role in optimizing engine performance, reducing fuel consumption, and consequently curbing greenhouse gas emissions. Such initiatives align with the broader objective of sustainability and environmental stewardship in the realm of power generation.

The percentage of NO_x emissions is relatively small, approximately 0.2% in the mass ratio of total GHG, but it can have detrimental effects on the environment. Therefore, NO_x emissions are predicted and plotted in Figures 16 and 17, using manufacturer data provided earlier in Figure 3. Figure 3 illustrates that the NO_x emission decreases with increasing ambient temperature, as per the manufacturer's description. As outlined by Pavri and Moore [47], engine manufacturers employ a typical exhaust temperature control curve. This curve is strategically crafted to maintain a constant turbine firing temperature within an ambient temperature span of 15 °C to 32 °C. However, when subjected to extreme ambient temperatures, the firing temperature is changed by engine control. At an ambient temperature of −18 °C, the curve leads to an under-firing situation of about 11 °C. Similarly, at an ambient temperature of 49 °C, the under-firing amounts to approximately 6 °C. Consequently, adopting lower firing temperatures in situations of elevated ambient temperatures contributes to a reduction in NO_x emissions, as elucidated.

In parallel to the discussion above, the calculations presented in Figure 16 demonstrate that when the engine inlet temperature is maintained at a constant 15 °C through inlet air cooling, the NO_x emissions remain constant. However, in the uncooled inlet air scenario, the engine control system lowers firing temperatures at high ambient temperatures, which can reduce NO_x emissions with respect to the 15 °C standard day condition. In the cooled inlet air scenario, the NO_x emissions will be constant (no reduction) due to the constant firing temperature at 15 °C constant inlet air temperature. Therefore, inlet air cooling keeps the NO_x emissions constant, but this situation can be considered an increase in NO_x compared to a reduction in NO_x at high ambient temperatures due to under-firing (Figure 17).

Finally, the effect of inlet air cooling on total CO₂-equivalent GHG emissions is investigated. Similarly, inlet air cooling systems bring important benefits for greenhouse gas (GHG) emission reduction. Again, at 55 °C without cooling, total GHG emissions (which are the sum of CO₂ and NO_x) increase by 5.84%, primarily due to increased fuel

consumption in the engine. However, when the refrigeration or cooling system in the inlet is activated, the increase in GHG emissions drops from 5.84% to 3.41%, which is an improvement of 2.43% in the GHG emissions on a 55 °C hot day (Figures 18 and 19).

4. Conclusions

The study presented calculations on the effects of utilizing inlet air cooling on a land-based gas turbine engine across a wide range of ambient temperatures (15–55 °C). A mechanical chiller was proposed to maintain a constant 15 °C inlet temperature by utilizing a portion of the engine's output power for cooling/refrigerating the inlet air. Inlet air cooling was found to be highly effective in recovering most of the power output losses at 55 °C, reducing performance degradation significantly. The rise in PSFC at 55 °C was mitigated by inlet air cooling, resulting in a notable improvement in fuel efficiency. These findings provided valuable insights for potential future implementations and highlighted the potential of inlet air cooling as an effective approach to mitigate the performance degradation and environmental impact of land-based gas turbine engines operating in hot weather conditions. By reducing power losses, improving fuel efficiency, and decreasing GHG emissions, inlet air cooling offered a viable solution to enhance overall engine performance and contribute to environmental sustainability. Further research and implementation efforts in this area can potentially lead to significant advancements in gas turbine technology and its environmental footprint.

The study also highlighted the favorable impact of inlet air cooling on heat rate and thermal efficiency, aiding in the recovery of engine efficiency under hot ambient conditions. Inlet air cooling demonstrated its potential for reducing CO₂ emissions by decreasing fuel consumption, as well as its relation to water vapor (H₂O) emissions during combustion. The study further addressed the relatively small but detrimental effects of NO_x emissions on the environment and their relationship to ambient temperature. Thus, inlet air cooling showed significant benefits in reducing total GHG emissions, emphasizing its potential contribution to emissions reduction strategies.

Overall, the study provided valuable insights into the benefits of utilizing inlet air cooling to mitigate the negative effects of high ambient temperatures on engine performance and emissions. Inlet air cooling offered a promising solution to enhance overall engine performance and contribute to environmental sustainability. Further research and implementation efforts in this area hold the potential for significant advancements in gas turbine technology and its environmental impact on power generation.

Author Contributions: Conceptualization, A.D.; methodology, A.D.; software, A.D.; validation, A.D.; formal analysis, A.D.; investigation, A.D.; data curation, A.D.; writing—original draft preparation, A.D.; writing—review and editing, A.D., A.M., E.T.D., F.A., I.E., K.N., M.M., M.F., M.O. and Y.G.; visualization, A.D.; supervision, A.D.; project administration, A.D. All authors have read and agreed to the published version of the manuscript.

Funding: This research received no external funding.

Data Availability Statement: The data presented in this study are available on request from the corresponding author. The data are not publicly available due to privacy.

Acknowledgments: The authors would like to thank American University of the Middle East, Kuwait, and colleagues Hasan Mulki, Mohamed Abouelela, and Askhat Mussin for their support on this study.

Conflicts of Interest: The authors declare no conflict of interest.

Nomenclature

CO_2	carbon dioxide
COP	coefficient of performance
EI	emission index (g/kg fuel)
GT	gas turbine
GWP	global warming potential
GHG	greenhouse gas
h	enthalpy (kJ/kg)
H_2O	water vapor
HR	heat rate
LHV	lower heating value of fuel (MJ/kg)
\dot{m}_a	inlet corrected air mass flow rate (kg/s)
\dot{m}_f	fuel mass flow rate (kg/s)
\dot{m}_T	air and fuel mass flow rate entering the turbine (kg/s)
Nox	nitrogen oxides
P_{amb}	ambient pressure (kPa)
$PSFC$	power-specific fuel consumption
\dot{Q}_{cool}	cooling load (kJ)
\dot{Q}_{in}	heat of fuel in the combustor (kJ)
T	total temperature at engine stations (K)
T_{amb}	ambient temperature (K)
\dot{W}_C	power of the compressor
\dot{W}_{cool}	work input for the mechanical chiller
\dot{W}_T	power of the turbine
\dot{W}_{net}	net shaft power delivered
Greek symbols	
η_{th}	thermal efficiency
η_b	burner efficiency

References

1. GE News GE's Gas Turbine Upgrades Increase Output and Efficiency at Kuwait's Sabiya West CCGT 2000 MW Power Plant. Available online: <https://www.ge.com/news/press-releases/ge/T1\textquoterights-gas-turbine-upgrades-increase-output-and-efficiency-kuwait/T1\textquoterights-sabiya-west-ccgt> (accessed on 12 October 2022).
2. KISR (Kuwait Institute for Scientific Research). Kuwait Energy Outlook. 2019. Available online: <https://www.undp.org/arab-states/publications/kuwait-energy-outlook-1> (accessed on 12 October 2022).
3. Brooks, F.J. *GE Gas Turbine Performance Characteristics*; GER-3567H; GE Power Systems: Schenectady, NY, USA, 2000.
4. De Sa, A.; Al Zubaidy, S. Gas Turbine Performance at Varying Ambient Temperature. *Appl. Therm. Eng.* **2011**, *31*, 2735–2739. [CrossRef]
5. Arabi, S.M.; Ghadamian, H.; Aminy, M.; Ozgoli, H.A.; Ahmadi, B.; Khodsiani, M. The Energy Analysis of GE-F5 Gas Turbines Inlet Air-Cooling Systems by the off-Design Method. *Meas. Control* **2019**, *52*, 1489–1498. [CrossRef]
6. Barigozzi, G.; Perdichizzi, A.; Gritti, C.; Guaiatelli, I. Techno-Economic Analysis of Gas Turbine Inlet Air Cooling for Combined Cycle Power Plant for Different Climatic Conditions. *Appl. Therm. Eng.* **2015**, *82*, 57–67. [CrossRef]
7. Bassily, A. Performance Improvements of the Intercooled Reheat Recuperated Gas-Turbine Cycle Using Absorption Inlet-Cooling and Evaporative after-Cooling. *Appl. Energy* **2004**, *77*, 249–272. [CrossRef]
8. Chase, D.L.; Kehoe, P.T. *GE Combined-Cycle Product Line and Performance*; GE Power Systems: Schenectady, NY, USA, 2000.
9. Chen, L.; Zhang, W.; Sun, F. Performance Optimization for an Open-Cycle Gas Turbine Power Plant with a Refrigeration Cycle for Compressor Inlet Air Cooling. Part 1: Thermodynamic Modelling. *Proc. Inst. Mech. Eng. Part A J. Power Energy* **2009**, *223*, 505–513. [CrossRef]
10. De Lucia, M.; Lanfranchi, C.; Boggio, V. Benefits of Compressor Inlet Air Cooling for Gas Turbine Cogeneration Plants. *J. Eng. Gas Turbines Power* **1996**, *118*, 598–603. [CrossRef]
11. Farzaneh-Gord, M.; Deymi-Dashtebayaz, M.; Hashemi-Marghzar, S. Improving the Efficiency of an Industrial Gas Turbine by a Novel Inlet Air Cooling Method. *J. Energy Inst.* **2009**, *82*, 150–158. [CrossRef]
12. GE Gas Power Inlet Air Chilling System. Available online: <https://www.ge.com/gas-power/services/gas-turbines/upgrades/inlet-air-chilling-system> (accessed on 14 October 2022).
13. Stellar Energy Turbine Inlet Air Chilling. Available online: <http://www.stellar-energy.net/what-we-do/solutions/turbine-inlet-air-chilling.aspx> (accessed on 14 October 2022).
14. Kodituwakku, D.R. *Effect of Cooling Charge Air on the Gas Turbine Performance and Feasibility of Using Absorption Refrigeration in the "Kelanitissa" Power Station, Sri Lanka*; KTH School of Industrial Engineering and Management: Stockholm, Sweden, 2021.

15. Loud, R.L.; Slaterpryce, A.A. *Gas Turbine Inlet Air Treatment*; GER-3419A; GE Power Generation: Schenectady, NY, USA, 1991.
16. Johnston, J.R. *Performance and Reliability Improvements for Heavy-Duty Gas Turbines*; GER-3571H; GE Power Systems: Schenectady, NY, USA, 2000.
17. Malewski, W.F.; Holldorff, G.M. Power Increase of Gas Turbines by Inlet Air Pre-Cooling With Absorption Refrigeration Utilizing Exhaust Waste Heat. In *Turbo Expo: Power for Land, Sea, and Air*; American Society of Mechanical Engineers: New York, NY, USA, 1986; pp. 1–4.
18. Mohapatra, A.K. Sanjay Comparative Analysis of Inlet Air Cooling Techniques Integrated to Cooled Gas Turbine Plant. *J. Energy Inst.* **2015**, *88*, 344–358. [\[CrossRef\]](#)
19. Najjar, Y.S.H. Enhancement of Performance of Gas Turbine Engines by Inlet Air Cooling and Cogeneration System. *Appl. Therm. Eng.* **1996**, *16*, 163–173. [\[CrossRef\]](#)
20. Najjar, Y.S.H.; Al-Zoghool, Y.M.A. Sustainable Energy Development in Power Generation by Using Green Inlet-Air Cooling Technologies with Gas Turbine Engines. *J. Eng. Thermophys.* **2015**, *24*, 181–204. [\[CrossRef\]](#)
21. Omar Kamal, S.N.; Salim, D.A.; Mohd Fouzi, M.S.; Hong Khai, D.T.; Yusri Yusof, M.K. Feasibility Study of Turbine Inlet Air Cooling Using Mechanical Chillers in Malaysia Climate. *Energy Procedia* **2017**, *138*, 558–563. [\[CrossRef\]](#)
22. Potnis, S.V.; Joshi, N.D. Turbine Inlet Air-Cooling System and Method. U.S. Patent 6,837,056 B2, 4 January 2005.
23. Rahim, M.A. Performance and Sensitivity Analysis of a Combined Cycle Gas Turbine Power Plant by Various Inlet Air-Cooling Systems. *Proc. Inst. Mech. Eng. Part A J. Power Energy* **2012**, *226*, 922–931. [\[CrossRef\]](#)
24. Sanaye, S.; Fardad, A.; Mostakhdemi, M. Thermoeconomic Optimization of an Ice Thermal Storage System for Gas Turbine Inlet air cooling. *Energy* **2011**, *36*, 1057–1067. [\[CrossRef\]](#)
25. Wang, F.J.; Chiou, J.S. Integration of Steam Injection and Inlet Air Cooling for a Gas Turbine Generation System. *Energy Convers. Manag.* **2004**, *45*, 15–26. [\[CrossRef\]](#)
26. Yang, C.; Yang, Z.; Cai, R. Analytical Method for Evaluation of Gas Turbine Inlet Air Cooling in Combined Cycle Power Plant. *Appl. Energy* **2009**, *86*, 848–856. [\[CrossRef\]](#)
27. Zurigat, Y.H.; Dawoud, B.; Bortmany, J. On the Technical Feasibility of Gas Turbine Inlet Air Cooling Utilizing Thermal Energy Storage. *Int. J. Energy Res.* **2006**, *30*, 291–305. [\[CrossRef\]](#)
28. Dinc, A. Optimization of Turboprop ESFC and NOx Emissions for UAV Sizing. *Aircr. Eng. Aerosp. Technol.* **2017**, *89*, 375–383. [\[CrossRef\]](#)
29. Dinc, A.; Elbadawy, I. Global Warming Potential Optimization of a Turbofan Powered Unmanned Aerial Vehicle during Surveillance Mission. *Transp. Res. Part D Transp. Environ.* **2020**, *85*, 102472. [\[CrossRef\]](#)
30. Dinc, A. The Effect of Flight and Design Parameters of a Turbofan Engine on Global Warming Potential. *IOP Conf. Ser. Mater. Sci. Eng.* **2021**, *1051*, 012051. [\[CrossRef\]](#)
31. Dinc, A.; Otkur, M. Emissions Prediction of an Aero-Piston Gasoline Engine during Surveillance Flight of an Unmanned Aerial Vehicle. *Aircr. Eng. Aerosp. Technol.* **2021**, *93*, 462–472. [\[CrossRef\]](#)
32. Dinc, A.; Gharbia, Y. Global Warming Potential Estimations of a Gas Turbine Engine and Effect of Selected Design Parameters. In *Proceedings of the ASME 2020 International Mechanical Engineering Congress and Exposition Volume 8: Energy, Virtual*, 16–19 November 2020; American Society of Mechanical Engineers: New York, NY, USA, 2020; Volume 8, pp. 1–7.
33. Dinc, A.; Taher, R.; Derakhshandeh, J.F.; Fayed, M.; Elbadawy, I.; Gharbia, Y. Performance Degradation of a 43 MW Class Gas Turbine Engine in Kuwait Climate. *Int. Res. J. Innov. Eng. Technol.* **2021**, *5*, 108–113. [\[CrossRef\]](#)
34. Dinc, A.; Elbadawy, I.; Fayed, M.; Taher, R.; Derakhshandeh, J.F.; Gharbia, Y. Performance Improvement of a 43 MW Class Gas Turbine Engine with Inlet Air Cooling. *Int. J. Emerg. Trends Eng. Res.* **2021**, *9*, 539–544. [\[CrossRef\]](#)
35. Machrafi, H. *Global Warming*; Dincer, I., Hepbasli, A., Midilli, A., Karakoc, T.H., Eds.; Green Energy and Technology; Springer: Boston, MA, USA, 2010; ISBN 978-1-4419-1016-5.
36. Dinc, A.; Caliskan, H.; Ekici, S.; Sohret, Y. Thermodynamic-Based Environmental and Enviroeconomic Assessments of a Turboprop Engine Used for Freight Aircrafts under Different Flight Phases. *J. Therm. Anal. Calorim.* **2022**, *147*, 12693–12707. [\[CrossRef\]](#)
37. Dinc, A. NOx Emissions of Turbofan Powered Unmanned Aerial Vehicle for Complete Flight Cycle. *Chin. J. Aeronaut.* **2020**, *33*, 1683–1691. [\[CrossRef\]](#)
38. Arias Quintero, S.; Auerbach, S.; Randel, J.; Kraft, R. Reduction in Greenhouse Gas Emissions in the Power Industry Using Compressed Air Power Enhancement Technology in Gas Turbines. In *Proceedings of the ASME Turbo Expo 2014: Turbine Technical Conference and Exposition*, Düsseldorf, Germany, 16–20 June 2014; Volume 3A, pp. 1–7. [\[CrossRef\]](#)
39. Walsh, P.P.; Fletcher, P. *Gas Turbine Performance*, 2nd ed.; John Wiley & Sons: Hoboken, NJ, USA, 2004; ISBN 063206434X.
40. Khan, R.S.R.; Barreiro, J.; Lagana, M.C.; Kyprianidis, K.G.; Ogaji, S.O.T.; Pilidis, P.; Bennett, I. An Assessment of the Emissions and Global Warming Potential of Gas Turbines for LNG Applications. In *Proceedings of the Volume 4: Cycle Innovations, Industrial and Cogeneration, Manufacturing Materials and Metallurgy*, Marine, Orlando, FL, USA, 8–12 June 2009; American Society of Mechanical Engineers Digital Collection: New York, NY, USA, 2009; pp. 123–132.
41. Svensson, F.; Hasselrot, A.; Moldanova, J. Reduced Environmental Impact by Lowered Cruise Altitude for Liquid Hydrogen-Fuelled Aircraft. *Aerosp. Sci. Technol.* **2004**, *8*, 307–320. [\[CrossRef\]](#)
42. Lawrence, M.G.; Crutzen, P.J. Influence of NOx Emissions from Ships on Tropospheric Photochemistry and Climate. *Nature* **1999**, *402*, 167–170. [\[CrossRef\]](#)
43. Lasek, J.A.; Lajnert, R. On the Issues of NOx as Greenhouse Gases: An Ongoing Discussion. ... *Appl. Sci.* **2022**, *12*, 10429. [\[CrossRef\]](#)
44. Lammel, G.; Graßl, H. Greenhouse Effect of NOx. *Environ. Sci. Pollut. Res.* **1995**, *2*, 40–45. [\[CrossRef\]](#)

45. IPCC Summary for Policymakers. *Climate Change 2014: Synthesis Report. Contribution of Working Groups I, II and III to the Fifth Assessment Report of the Intergovernmental Panel on Climate Change*; Core Writing Team, Pachauri, R.K., Meyer, L.A., Eds.; IPCC: Geneva, Switzerland, 2014.
46. Dominguez-Ramos, A.; Irabien, A. The Carbon Footprint of Power-to-Synthetic Natural Gas by Photovoltaic Solar Powered Electrochemical Reduction of CO₂. *Sustain. Prod. Consum.* **2019**, *17*, 229–240. [[CrossRef](#)]
47. Pavri, R.; Moore, G.D. *Gas Turbine Emissions and Control*; GER-4211; GE Power Systems: Atlanta, GA, USA, 2001.
48. Hung, W.S.Y. A Predictive NO_x Monitoring System for Gas Turbines. In *Proceedings of the Volume 3: Coal, Biomass and Alternative Fuels, Combustion and Fuels, Oil and Gas Applications, Cycle Innovations*, Orlando, FL, USA, 3–6 June 1991; American Society of Mechanical Engineers: New York, NY, USA, 1991.

Disclaimer/Publisher’s Note: The statements, opinions and data contained in all publications are solely those of the individual author(s) and contributor(s) and not of MDPI and/or the editor(s). MDPI and/or the editor(s) disclaim responsibility for any injury to people or property resulting from any ideas, methods, instructions or products referred to in the content.